

## Ultraviolet electroluminescence from ordered ZnO nanorod array/p-GaN light emitting diodes

J. J. Dong, X. W. Zhang, Z. G. Yin, J. X. Wang, S. G. Zhang et al.

Citation: *Appl. Phys. Lett.* **100**, 171109 (2012); doi: 10.1063/1.4706259

View online: <http://dx.doi.org/10.1063/1.4706259>

View Table of Contents: <http://apl.aip.org/resource/1/APPLAB/v100/i17>

Published by the [American Institute of Physics](#).

---

### Related Articles

Transparent Ti-In-Sn-O multicomponent anodes for highly efficient phosphorescent organic light emitting diodes  
*J. Appl. Phys.* **112**, 023513 (2012)

Au nanoparticle-decorated graphene electrodes for GaN-based optoelectronic devices  
*Appl. Phys. Lett.* **101**, 031115 (2012)

Blue light emitting diode internal and injection efficiency  
*AIP Advances* **2**, 032117 (2012)

Buried graphene electrodes on GaN-based ultra-violet light-emitting diodes  
*Appl. Phys. Lett.* **101**, 031108 (2012)

Nitrogen-polar core-shell GaN light-emitting diodes grown by selective area metalorganic vapor phase epitaxy  
*Appl. Phys. Lett.* **101**, 032103 (2012)

---

### Additional information on *Appl. Phys. Lett.*

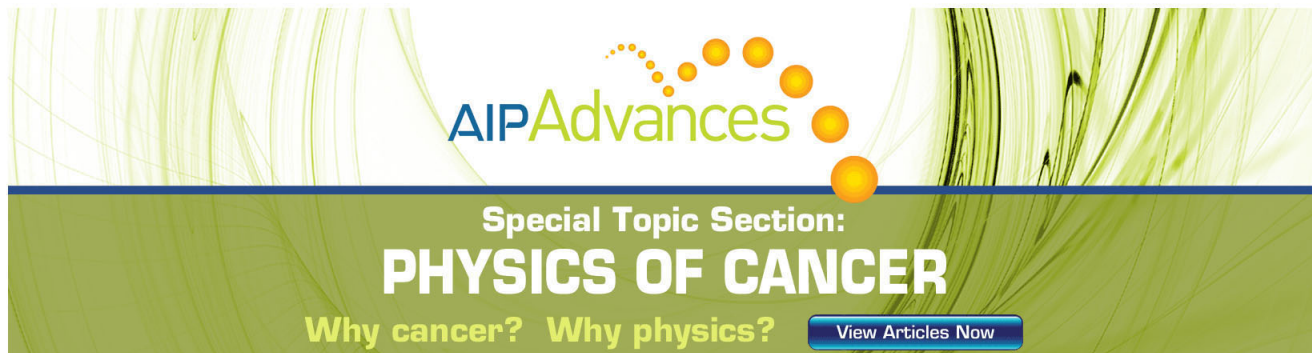
Journal Homepage: <http://apl.aip.org/>

Journal Information: [http://apl.aip.org/about/about\\_the\\_journal](http://apl.aip.org/about/about_the_journal)

Top downloads: [http://apl.aip.org/features/most\\_downloaded](http://apl.aip.org/features/most_downloaded)

Information for Authors: <http://apl.aip.org/authors>

## ADVERTISEMENT

The advertisement features a green and white background with abstract, flowing lines. At the top, the 'AIP Advances' logo is displayed in green and yellow. Below it, the text 'Special Topic Section: PHYSICS OF CANCER' is written in white on a dark green background. At the bottom, the phrase 'Why cancer? Why physics?' is written in white, followed by a blue button with the text 'View Articles Now' in white.

AIP Advances

Special Topic Section:  
**PHYSICS OF CANCER**

Why cancer? Why physics? [View Articles Now](#)

## Ultraviolet electroluminescence from ordered ZnO nanorod array/p-GaN light emitting diodes

J. J. Dong,<sup>1</sup> X. W. Zhang,<sup>1,a)</sup> Z. G. Yin,<sup>1</sup> J. X. Wang,<sup>2</sup> S. G. Zhang,<sup>1</sup> F. T. Si,<sup>1</sup> H. L. Gao,<sup>1</sup> and X. Liu<sup>1</sup>

<sup>1</sup>Key Lab of Semiconductor Materials Science, Institute of Semiconductors, CAS, Beijing 100083, People's Republic of China

<sup>2</sup>Semiconductor Lighting Technology R&D Center, Institute of Semiconductors, CAS, Beijing 100083, People's Republic of China

(Received 20 March 2012; accepted 6 April 2012; published online 25 April 2012)

The highly ordered and aligned ZnO nanorod arrays were grown on p-GaN substrates via a facile hydrothermal process assisted by the inverted self-assembled monolayer template, from which the ZnO nanorod/p-GaN heterojunction light emitting diodes (LEDs) were fabricated. The ZnO nanorod-based LEDs exhibit a stronger ultraviolet emission of 390 nm than the ZnO film-based counterpart, which is attributed to the low density of interfacial defects, the improved light extraction efficiency, and carrier injection efficiency through the nano-sized junctions. Furthermore, the LED with the 300 nm ZnO nanorods has a better electroluminescence performance compared with the device with the 500 nm nanorods. © 2012 American Institute of Physics. [<http://dx.doi.org/10.1063/1.4706259>]

Wurtzite ZnO is regarded as one of the most promising wide-bandgap semiconductor material for the application of ultraviolet (UV) light emitting diodes (LEDs) and laser diodes due to its excellent optical and electrical properties, including a direct wide bandgap of 3.37 eV and a high exciton binding energy of 60 meV. Because of the difficulty in achieving stable and reproducible p-type ZnO films and the similarity in the crystal structure and physical properties with ZnO, high-quality p-GaN has been widely used to construct the ZnO-based heterojunction LEDs.<sup>1</sup> In general, however, a p-n heterojunction device suffers a lower carrier injection efficiency than a homojunction structure, due to the large band offset formed at the junction interface. This problem can be overcome by introducing ZnO nanostructure to increase the carrier injection rate through nanojunction.<sup>2,3</sup> Moreover, one-dimensional (1D) ZnO nanostructures such as nanorods have high crystalline quality, excellent waveguiding properties, and simple fabrication process. Therefore, n-ZnO nanorods/p-GaN film heterojunction LEDs have attracted considerable attention, and many types of heterojunction LEDs based on 1D ZnO nanostructures and p-GaN substrates have been investigated.<sup>2-9</sup> Among these structures, the heterojunction LEDs using highly ordered and vertically aligned ZnO nanorod arrays, which can bring about improved performance of multifunctional devices and systems, are the most attractive. Compared with random-distributed ZnO nanostructures, the ordered ZnO nanorod arrays have a lower defect density,<sup>10</sup> an improvement in the light extraction efficiency of the LEDs,<sup>11</sup> and a broadband suppression in reflection.<sup>12</sup> In addition, the patterned ZnO nanostructure arrays can form a two-dimensional photonic crystal, then one can match the wavelength of the emitted light to the bandgap of the photonic crystal by controlling the periodicity of the nanostructure arrays, possibly resulting

in normal directional emission of the light.<sup>13</sup> However, so far, the LEDs based on the ordered ZnO nanowire/nanorod arrays have only been achieved, assisted by electron beam lithography (EBL),<sup>13</sup> which is too costly and time consuming to be practical. As an alternative, self-assembled nanosphere lithography (NSL), which employs self-assembled monolayer (SAM) colloidal crystals as the mask to create a patterned seed layer or substrate to guide the growth of nanostructures, has been proven to be a simple and cost-effective technique for the patterning of nanostructure arrays with long-range periodicity in a large scale.<sup>14,15</sup>

In this letter, the highly ordered and aligned ZnO nanorod arrays were grown on p-GaN substrates via a facile hydrothermal process assisted by the inverted SAM template, from which the ZnO nanorods/p-GaN heterojunction LEDs were fabricated. Both diameter and density of ZnO nanorods were tuned by using the polystyrene (PS) microspheres with different sizes and varying the solution concentration during hydrothermal growth, and the electroluminescence (EL) performance of these ordered ZnO nanorod-based LEDs was investigated. It is found that the ZnO nanorod-based LEDs exhibit a stronger UV emission of ~390 nm compared with the ZnO film-based counterpart. This work provides a route for developing high performance optoelectronic devices based on ZnO nanorods.

Highly ordered and vertically aligned ZnO nanorod arrays on the p-GaN substrates were achieved via a hydrothermal route by using the TiO<sub>2</sub> ring template deriving from the PS microsphere SAM, which has been described detailedly in our previous report.<sup>16</sup> Herein, the PS microspheres with diameter of 500 nm and 1 μm were used to adjust the density of ZnO nanorods. To grow the ZnO nanorod arrays by the hydrothermal process, the aqueous solutions of Zn(NO<sub>3</sub>)<sub>2</sub>·6H<sub>2</sub>O and hexamethylenetetramine (HMTA) with the identical concentration were used. The diameters of ZnO nanorods were tuned by varying the solution concentration during hydrothermal growth instead of reactive ion

<sup>a)</sup>Author to whom correspondence should be addressed. Electronic mail: xwzhang@semi.ac.cn.

etching (RIE) of PS microspheres. For the fabrication of ZnO nanorod-based LEDs, the as-grown ZnO nanorod arrays were spin-coated with poly(methyl methacrylate) (PMMA) to protect the nanorods and to isolate electrical contacts on the ZnO nanorods from the p-GaN substrate. Then, an oxygen plasma etching was used to remove the PMMA coated on the surface of ZnO nanorods and expose the nanorod tips. Next, a 100 nm indium-tin-oxide (ITO) film for current spreading was deposited by radio-frequency (RF) magnetron sputtering. Finally, Ni/Au contacts were thermally evaporated onto the p-GaN substrates and Ti/Au contacts onto the exposed ZnO nanorod tips. Surface morphologies of the samples were characterized by atomic force microscopy (AFM, NT-MDT Solver P47) and scanning electron microscopy (SEM, Hitachi FE-S4800). The EL measurements of ZnO-based LEDs were carried out at room temperature (RT) using a Hitachi F4500 fluorescence spectrophotometer. The photoluminescence (PL) spectra were acquired by exciting with a 325 nm He-Cd laser with a power of 30 mW at RT.

Controlling the diameter, density, and length of ZnO nanorod array is essential for advanced photonic optical devices.<sup>17</sup> It has been demonstrated in our previous work<sup>16</sup> that the diameter of ZnO nanorods can be tuned over a wide range by varying the time of oxygen RIE of PS microspheres. However, RIE is a costly and complex process, and moreover, the plasma may induce damage of GaN substrates which will lead to the degradation of the electrical properties of LEDs. So herein, the diameters of ZnO nanorods were tuned by varying the solution concentration during hydrothermal growth. As shown in Figs. 1(a) and 1(b), the ZnO nanorods with diameters of 400 and 300 nm were obtained at 50 °C for 6 h with the solution concentrations of 0.075 M and 0.035 M, respectively, for the 500 nm PS microspheres in use. The ZnO nanorod arrays have hexagonal periodicity and evenly distribution inheriting from the PS microsphere SAM, and all the ZnO nanorods are hexagonal-faceted with uniform diameter and height. Besides, the perfect epitaxial growth of ZnO nanorods on GaN along [0001] was confirmed by the x-ray diffraction (XRD) measurements.<sup>16</sup> It

should be noted that a relatively high solution concentration is essential for the growth of the individual ZnO nanorod array due to the faster feeding of the reactant ions to the growth sites. When the solution concentration is decreased to 0.02 M, the ZnO nanorod bundles rather than the single nanorod from each growth site will be obtained.<sup>16</sup> To adjust the density of ZnO nanorods, the PS microspheres with diameter of 1  $\mu\text{m}$  were used, and the corresponding results are shown in Figs. 1(c) and 1(d). As can be seen, the diameter of ZnO nanorods is about 500 nm at the solution concentration of 0.05 M, and the spacing between two neighboring nanorods is 1  $\mu\text{m}$ , which is predetermined by the diameter of the PS microspheres. As a result, by varying the size of PS microspheres and the solution concentration of hydrothermal growth, both the diameter and the density of ZnO nanorods have been tuned flexibly without an additional RIE process.

To guarantee the complete filling and moderate etching of PMMA, AFM measurements of the ZnO nanorod arrays were performed before and after filling of PMMA, as well as after plasma etching, and the corresponding AFM images are shown in Figs. 2(a)–2(c). Combined with the height profile (Fig. 2(d)) of the lines drawn in Figs. 2(a)–2(c), we can examine the process of each treatment precisely. For the as-grown ZnO nanorod arrays, the AFM image (Fig. 2(a)) presents a distinct individual hexagon array with a measured height of about 130 nm from the height profile, which is much lower than the actual height of the ZnO nanorods due to the geometric configuration of the scanning probe. Typically, the scanning probe has a pyramidal shape with a 10 nm tip curvature radius, and the probe size sharply increases from the tip to the root. Therefore, for the deep trenches in the samples, the scanning probe is partially blocked and cannot reach down to the bottom of the trenches. As a result, the measured height of ZnO nanorods by AFM is much lower than the actual value. After the filling of PMMA, the shape of individual nanorod becomes indistinguishable, and the surface of the sample gets flat as shown in the height profile, indicating that the ZnO nanorods have been wrapped with PMMA completely. Finally, after oxygen plasma etching for a certain time, the head parts of the nanorods are observed again and the height profile shows a small fluctuation of about 20 nm, which implies that the tips of the ZnO nanorods have been exposed while the spacing between two neighboring nanorods is still filled with PMMA.

The ZnO nanorods/p-GaN epitaxial heterostructure was then used to construct a LED device, and the schematic structure of device is illustrated in the inset of Fig. 3(a). The EL spectra for the device with the 300 nm ZnO nanorods under various currents ranging from 2 to 10 mA are shown in Fig. 3(a). These spectra exhibit a unique peak centered at about 390 nm, which has been observed frequently from the EL spectra of ZnO-based LEDs and can be attributed to the near-band-edge (NBE) emission from ZnO.<sup>18,19</sup> For comparison, a reference LED was fabricated based on a ZnO thin film and an AlN barrier layer,<sup>20</sup> and the corresponding EL spectra and its schematic structure are presented in Fig. 3(b). Obviously, the EL emission from the nanorod-based LED is stronger than that of the ZnO film-based device at all injection currents, which can be due to the low density of the interfacial defects and the improved carrier injection

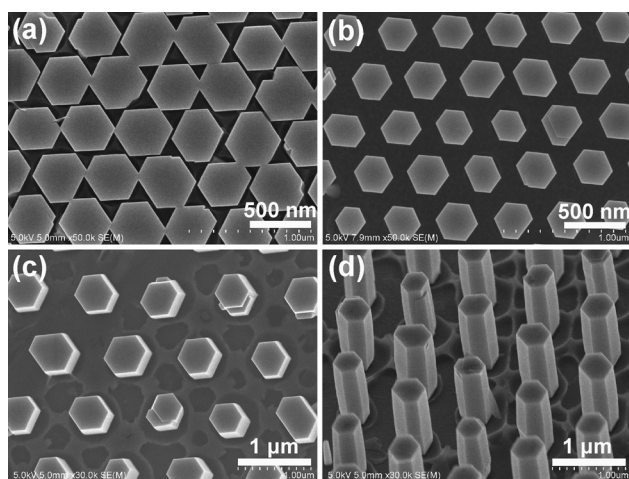


FIG. 1. Ordered and aligned ZnO nanorod arrays on the GaN substrates grown at 50 °C for 6 h with the reactant concentration of (a) 0.075 M and (b) 0.035 M by using 500 nm PS microspheres. (c) Top view and (d) 45° tilt view of the ZnO nanorod array on the GaN substrate grown at 0.05 M, 50 °C for 6 h by using 1  $\mu\text{m}$  PS microspheres.

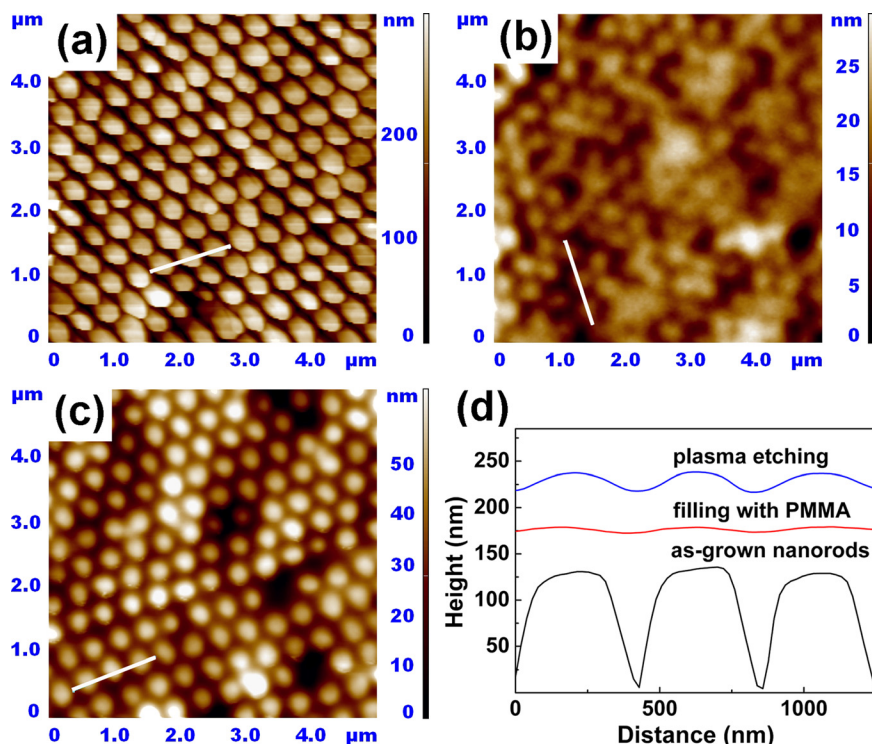


FIG. 2. AFM images of (a) the ZnO nanorod array, (b) the ZnO nanorod array after filling of PMMA and (c) after oxygen plasma etching of PMMA, and (d) the height profile of the lines drawn in Figs. 2(a)–2(c).

efficiency through the nanosized junctions.<sup>4,5</sup> Moreover, the increase in the light extraction efficiency of nanorod-based LEDs by virtue of the waveguiding properties of nanorods may also be responsible for the stronger EL peak, since the flat film-based LEDs may suffer from the low light extraction efficiency as limited by the total internal reflection. Besides, based on an effective medium theory, these graded refractive indices of GaN (2.49), ZnO (2.10), PMMA (1.59), and air (1.0) can largely reduce the Fresnel reflection between GaN/ZnO, ZnO/PMMA, and PMMA/air interfaces, which helps the optical transmission.<sup>13</sup>

The origin of the EL emission of heterojunction diodes was confirmed by comparing the EL and PL spectra. The PL spectrum of the ZnO thin film on the AlN/GaN substrate, as shown in Fig. 4(a), exhibits a dominant UV peak at 380 nm

along with a weak and broad visible emission band covering the range from 500 to 650 nm. The 380 nm UV emission is due to the NBE emission of ZnO, and the visible emission can be attributed to intrinsic defects such as oxygen vacancies ( $V_O$ ).<sup>4,18</sup> For the ZnO nanorod arrays on GaN substrates, the PL spectra present a unique UV emission of 380 nm, while the defect related visible emission cannot be almost observed, implying the high crystal quality of the ZnO nanorods on GaN substrates. Figure 4(b) presents the EL spectra of the LEDs based on ZnO nanorods with different diameters (300 and 500 nm) at the injection current of 6 mA, together with the EL spectrum of ZnO film-based LED at the same current. As can be seen, the EL spectra of all the three diodes

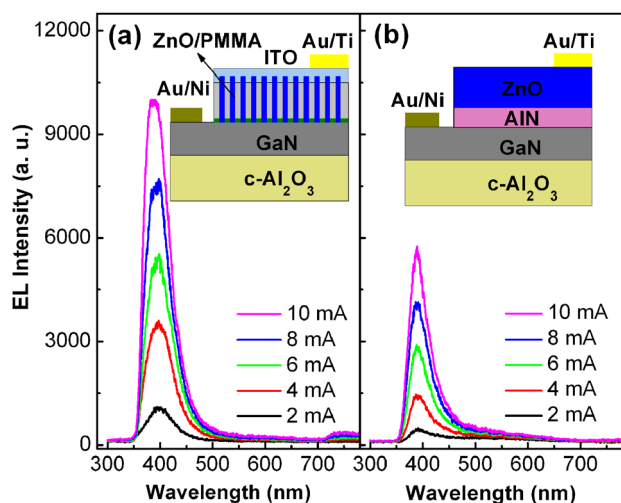


FIG. 3. EL spectra of (a) a ZnO nanorods/p-GaN LED and (b) a ZnO film-based LED under various currents ranging from 2 to 10 mA. The insets show the schematic structures of the corresponding LEDs, respectively.

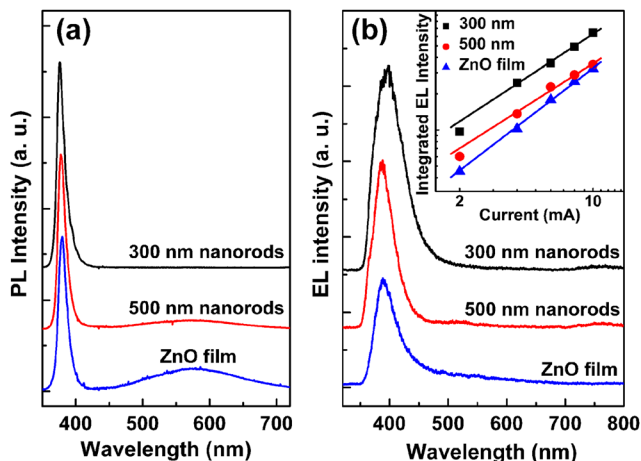


FIG. 4. (a) PL spectra of the ZnO thin film on the p-GaN substrate and the ZnO nanorods with different diameters. (b) EL spectra of the LEDs based on ZnO nanorods with different diameters at the injection current of 6 mA, together with the EL spectrum of ZnO film-based LED at the same current. The inset shows the integrated EL intensities of all the three devices as a function of the injection current. The solid line represents the fitting result based on the power law  $L = cI^m$ .

demonstrate a dominant emission at 390 nm, which is red-shifted by 10 nm with respect to the PL spectra. This phenomenon has been observed frequently for ZnO-based LEDs and could be interpreted tentatively in the following. On the one hand, it should be noted that there is some difference between PL and EL processes. The PL process depends on the recombination of nonequilibrium carriers in the surface layer, whereas the EL process is determined via the carrier recombination within the space charge region of heterojunction.<sup>21</sup> On the other hand, the junction heating effect under a constant injection current will cause band bending and lead to the red shift of EL peak.<sup>9,19</sup>

As expected, the emission from either of the ZnO nanorod-based diodes is stronger than that from the ZnO film-based device. Furthermore, the LED with the 300 nm nanorods has a better EL performance compared with the one with 500 nm ZnO nanorods. As mentioned earlier, one of the advantages of using the aligned nanorod array over the thin film is the enhanced light emission by the waveguiding effect of nanorods. An ideal single mode waveguide cavity would be around 220 nm for the ZnO nanorods surrounded by PMMA when the free space wavelength of the propagating light is 390 nm according to the EL peak in our experiments.<sup>22</sup> Therefore, the stronger EL emission from the device with the 300 nm ZnO nanorods can be attributed to their better waveguiding property, though it can be enhanced further by choosing an optimal diameter. In addition, the higher density of 300 nm ZnO nanorods may also contribute to the stronger EL emission.

To clarify the mechanism of the improved EL from nanorod-based LEDs, the integrated intensity of the EL peak as a function of the injection current in a log-log scale for all the three LEDs are plotted in the inset of Fig. 4(b). In agreement with the spectral evolution, the results can be fitted with the law  $L = cI^m$ , where  $m$  accounts for the influence of nonradiative defects in the characteristics of light emission.<sup>23</sup> A linear increase of  $L$  with  $I$  ( $m \sim 1$ ) can be expected as the radiative recombination dominates. When the nonradiation recombination becomes dominant,  $L$  shows a superline dependence on  $I$  ( $m > 1$ ).<sup>24</sup> For both of the nanorod-based LEDs, the curves show a linear dependence with  $m = 1.04$  and 1.01 for the 300 and 500 nm ZnO nanorods, respectively. This implies a negligible role of defect-related nonradiation recombination for the nanorod-based devices, which is in good agreement with the PL spectra and confirms again the high crystal quality of the ZnO nanorod arrays. However, the value of  $m$  determined from the fitting curve of ZnO film-based LED is 1.22, indicating the presence of nonradiative recombination centers in the space-charge region introduced by the interfacial defects. Since the low density of interfacial defects is favorable for improving carrier injection efficiency through the nanosize junctions, the ZnO nanorods/p-GaN heterojunction LEDs present improved EL performance compared with the ZnO film-based LEDs.

In conclusion, the ordered and aligned ZnO nanorod arrays were grown on p-GaN substrates via a facile hydrothermal process assisted by the inverted PS SAM template, and the ZnO nanorods/p-GaN epitaxial heterostructure was

used to construct a LED device. The nanorod-based LEDs exhibit significantly improved EL performance compared with the ZnO film-based counterpart, which is attributed to the low density of interfacial defects, the improved light extraction efficiency, and carrier injection efficiency through the nanosized junctions. Furthermore, the EL performance of the LEDs based on ZnO nanorods with different diameters was investigated. It is found that the LED with the 300 nm nanorods has a better EL performance than the device with 500 nm ZnO nanorods. This work will be helpful to the design of high efficiency and nanoscale UV LEDs.

This work was financially supported by the National Basic Research Program of China (Grant Nos. 2012CB934200 and 2012CB619306) and the National Natural Science Foundation of China (Grant Nos. 51071145 and 60876031).

- <sup>1</sup>Ya. I. Alivov, J. E. Van Nostrand, D. C. Look, M. V. Chukichev, and B. M. Ataev, *Appl. Phys. Lett.* **83**, 2943 (2003).
- <sup>2</sup>W. I. Park and G. C. Yi, *Adv. Mater.* **16**, 87 (2004).
- <sup>3</sup>M. C. Jeong, B. Y. Oh, M. H. Ham, and J. M. Myoung, *Appl. Phys. Lett.* **88**, 202105 (2006).
- <sup>4</sup>M. C. Jeong, B. Y. Oh, M. H. Ham, S. W. Lee, and J. M. Myoung, *Small* **3**, 568 (2007).
- <sup>5</sup>O. Lupan, T. Pauporte, and B. Viana, *Adv. Mater.* **22**, 3298 (2010).
- <sup>6</sup>J. J. Cole, X. Y. Wang, R. J. Knuesel, and H. O. Jacobs, *Nano Lett.* **8**, 1477 (2008).
- <sup>7</sup>X. M. Zhang, M. Y. Lu, Y. Zhang, L. J. Chen, and Z. L. Wang, *Adv. Mater.* **21**, 2767 (2009).
- <sup>8</sup>S. H. Park, S. H. Kim, and S. W. Han, *Nanotechnology* **18**, 055608 (2007).
- <sup>9</sup>T. C. Lu, M. Y. Ke, S. C. Yang, Y. W. Cheng, L. Y. Chen, G. J. Lin, Y. H. Lu, J. H. He, H. C. Kuo, and J. J. Huang, *Opt. Lett.* **35**, 4109 (2010).
- <sup>10</sup>C. Li, G. S. Hong, P. W. Wang, D. P. Yu, and L. M. Qi, *Chem. Mater.* **21**, 891 (2009).
- <sup>11</sup>H. Park, K. J. Byeon, K. Y. Yang, J. Y. Cho, and H. Lee, *Nanotechnology* **21**, 355304 (2010).
- <sup>12</sup>C. Cheng, M. Lei, L. Feng, T. L. Wong, K. M. Ho, K. K. Fung, M. M. T. Loy, D. P. Yu, and N. Wang, *ACS Nano* **3**, 53 (2009).
- <sup>13</sup>S. Xu, C. Xu, Y. Liu, Y. F. Hu, R. S. Yang, Q. Yang, J. Ryou, H. J. Kim, Z. Lochner, S. Choi, R. Dupuis, and Z. L. Wang, *Adv. Mater.* **22**, 4749 (2010).
- <sup>14</sup>J. Rybczynski, D. Banerjee, A. Kosior, M. Giersig, and Z. F. Ren, *Nano Lett.* **4**, 2037 (2004).
- <sup>15</sup>D. F. Liu, Y. J. Xiang, X. C. Wu, Z. X. Zhang, L. F. Liu, L. Song, X. W. Zhao, S. D. Luo, W. J. Ma, J. Shen, W. Y. Zhou, G. Wang, C. Y. Wang, and S. S. Xie, *Nano Lett.* **6**, 2375 (2006).
- <sup>16</sup>J. J. Dong, X. W. Zhang, Z. G. Yin, S. G. Zhang, J. X. Wang, H. R. Tan, Y. Gao, F. T. Si, and H. L. Gao, *ACS Appl. Mater. Interfaces* **3**, 4388 (2011).
- <sup>17</sup>K. S. Kim, H. Jeong, M. S. Jeong, and G. Y. Jung, *Adv. Funct. Mater.* **20**, 3055 (2010).
- <sup>18</sup>S. G. Zhang, X. W. Zhang, Z. G. Yin, J. X. Wang, J. J. Dong, H. L. Gao, F. T. Si, S. S. Sun, and Y. Tao, *Appl. Phys. Lett.* **99**, 181116 (2011).
- <sup>19</sup>O. Lupan, T. Pauporte, B. Viana, I. M. Tiginyanu, V. V. Ursaki, and R. Cortes, *ACS Appl. Mater. Interfaces* **2**, 2083 (2010).
- <sup>20</sup>J. B. You, X. W. Zhang, S. G. Zhang, J. X. Wang, Z. G. Yin, H. R. Tan, W. J. Zhang, P. K. Chu, B. Cui, A. M. Wowchak, A. M. Dabiran, and P. P. Chow, *Appl. Phys. Lett.* **96**, 201102 (2010).
- <sup>21</sup>S. G. Zhang, X. W. Zhang, Z. G. Yin, J. X. Wang, J. J. Dong, Z. G. Wang, S. Qu, B. Cui, A. M. Wowchak, A. M. Dabiran, and P. P. Chow, *J. Appl. Phys.* **109**, 093708 (2011).
- <sup>22</sup>K. S. Kim, S. M. Kim, H. Jeong, M. S. Jeong, and G. Y. Jung, *Adv. Funct. Mater.* **20**, 1076 (2010).
- <sup>23</sup>J. D. Ye, S. L. Gu, S. M. Zhu, W. Liu, S. M. Liu, R. Zhang, Y. Shi, and Y. D. Zheng, *Appl. Phys. Lett.* **88**, 182112 (2006).
- <sup>24</sup>S. G. Zhang, X. W. Zhang, J. X. Wang, J. B. You, Z. G. Yin, J. J. Dong, B. Cui, A. M. Wowchak, A. M. Dabiran, and P. P. Chow, *Phys. Status Solidi (RRL)* **5**, 74 (2011).